extract was diluted with the extracting medium as the ratio of 0.5, 0.25, 0.125, and 0.0625.

About 3.0×10^2 HEL299 cells were seeded in 100 μL of E-MEM with NEAA, 0.1 M Na-Pyr, 0.1% LAH, and 10 vol.% FBS into each well of a 96-well microplate. Based on the results of the pretests performed under the same procedure, the number of cells inoculated was determined. The same amount of the medium without cells was added to the blank well. The plate was kept for 20 min at room temperature before it was put into the CO_2 incubator in order to prevent the difference in cell growth of 36 outside wells to other inner wells. Then, cells were cultured for 4 h and a 100-μL portion of extracts or its diluted solutions was added into the well. The same amount of extracting medium unused to the dynamic extraction was added to the control well. Five concentrations were tested for each extract of three materials. Six replicate wells were prepared for each concentration of the extracts. After the second incubation of 9 days, the cells were fixed by 25% glutaraldehyde solution for 10 min and stained by 0.4% crystal violet solution in methanol for 30 min. The absorbance at 595nm was measured by a microplate reader. The relative viability of the cells (RVC) was calculated by the following equation:

$$\mathrm{RVC}(\%) = [(a-b)/(c-b)] \times 100$$

where a was the absorbance of the sample well, b was the absorbance of the blank well, and c was the absorbance of the control well.

The obtained RVC data were plotted as a function of the extract fraction to draw a "dose–response curve".

2.4. Quantitative analysis of metallic elements

The quantification of metallic elements in each extract of three specimens was performed by ICP-MS at Mitsui Chemical Analysis and Consulting Service. Quantification was performed for five metallic elements such as Cr, Fe, Mn, Mo, and Ni under the optimum condition for each element.

3. Results

3.1. Cytotoxicity test in static conditions

The microscopic images of the cells cultured on three disks sterilized by UV-irradiation for 1, 4, and 7 days are shown in Fig. 1 and their magnified images are shown in Fig. 2. After 1-day incubation, the cells were observed as scattered black dots because of the dye while the cells grew spread to cover almost all surface area of the disks of Fe–Cr–Mo and Fe–Cr–Mo–N after 7-day incubation. At the magnified images (Fig. 2), most of the cells were observed to spread along the polishing marks especially after 4- and 7-day incubations. The number of the cells on three disks was almost same after 1-day incubation whereas after 4- and

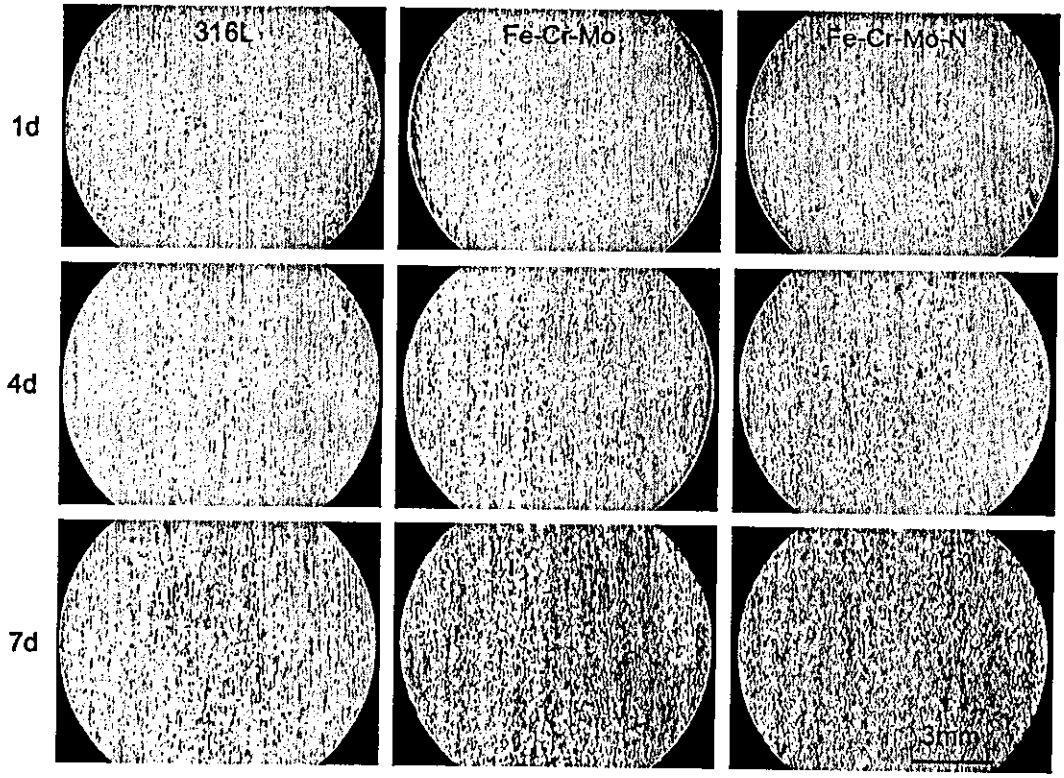

Fig. 1. Microscopic images of the cells cultured on the disks of 316L, Fe–Cr–Mo, and Fe–Cr–Mo–N sterilized by UV-irradiation.

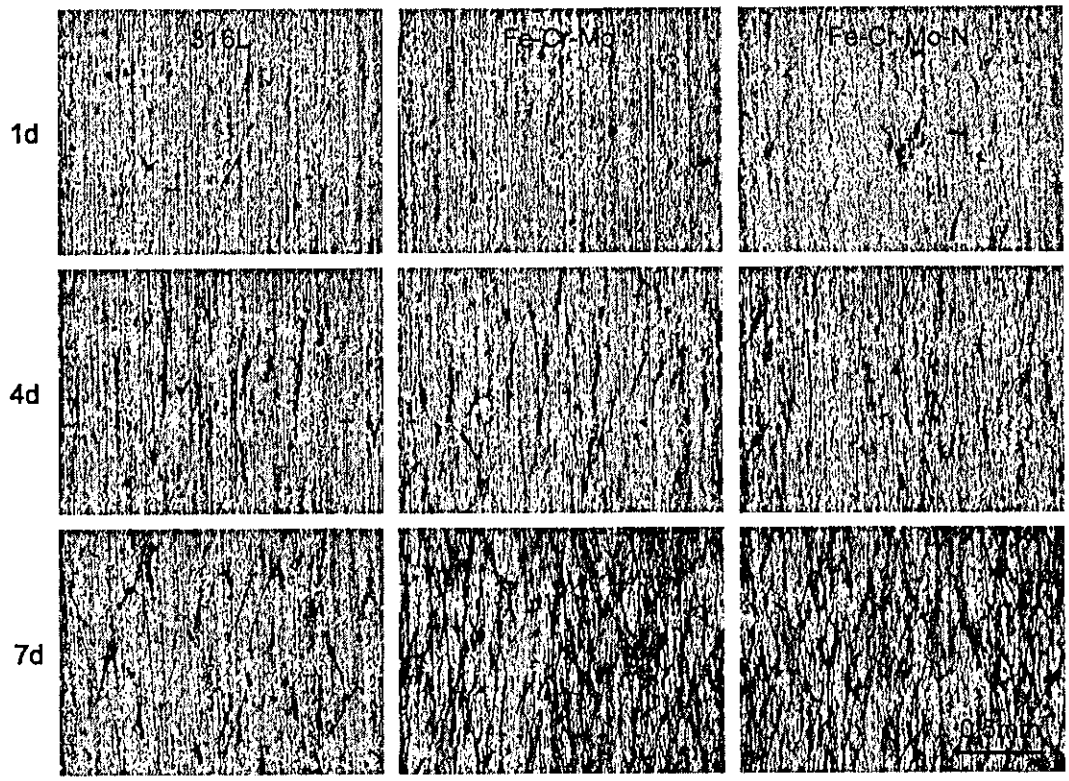

Fig. 2. Magnified images of the cells cultured on the disks of 316L, Fe–Cr–Mo, and Fe–Cr–Mo–N sterilized by UV-irradiation.

7-day incubations, the number of the cells on 316L was obviously smaller than Fe–Cr–Mo and Fe–Cr–Mo–N. The images of the cells cultured on three disks sterilized by autoclaving for 1, 4, and 7 days are shown in Fig. 3 as well as their magnified images are shown in Fig. 4. Again, the cells were scattered dots on the disks after 1-day incubation,

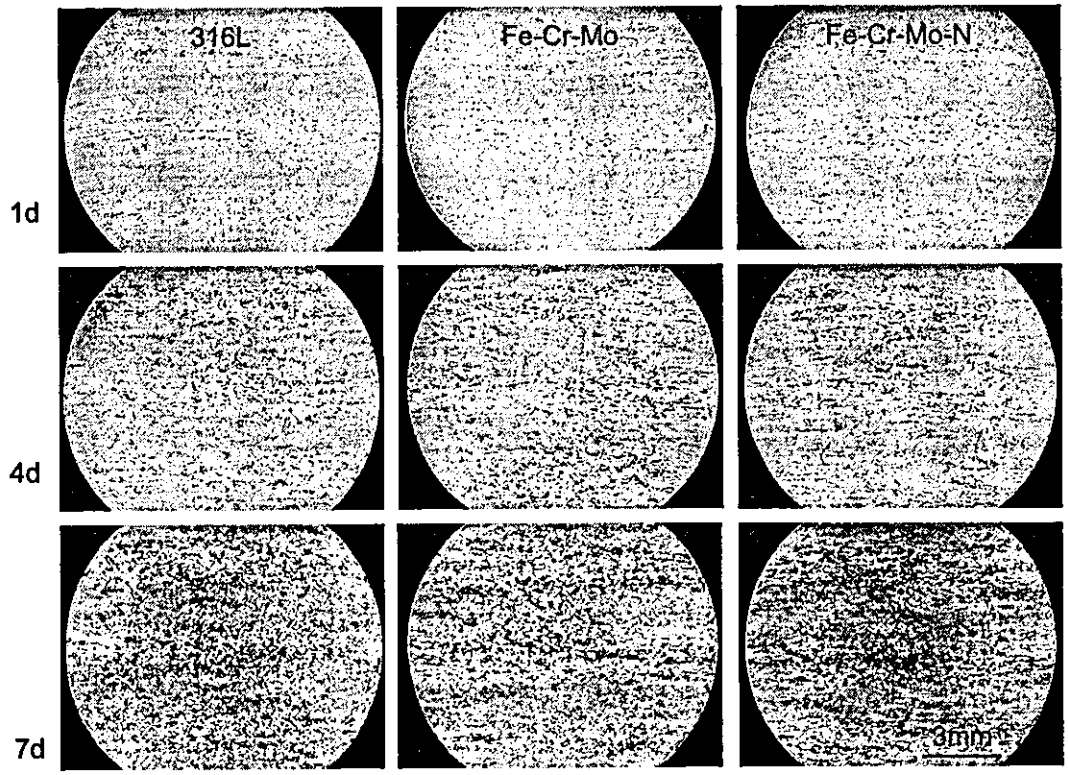

Fig. 3. Microscopic images of the cells cultured on the disks of 316L, Fe–Cr–Mo, and Fe–Cr–Mo–N sterilized by autoclaving.

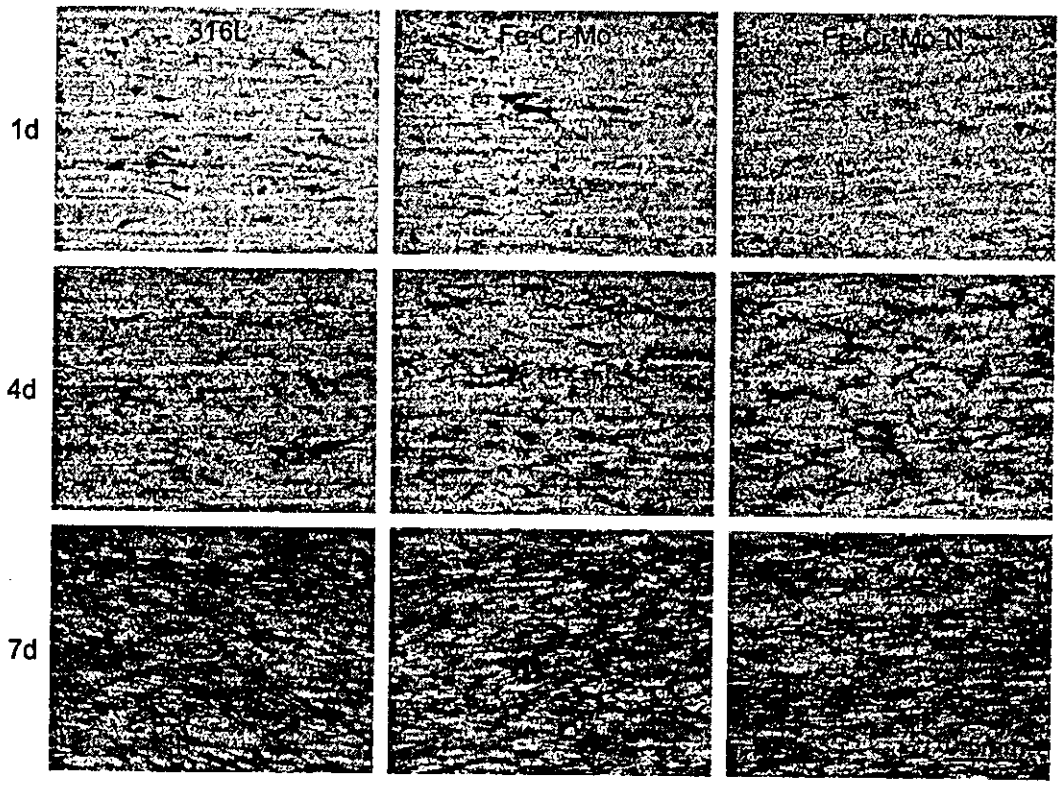

Fig. 4. Magnified images of the cells cultured on the disks of 316L, Fe–Cr–Mo, and Fe–Cr–Mo–N sterilized by autoclaving.

whereas they grew and covered the most of the disks after 7-day incubation. The magnified images (Fig. 4) showed the tendency that the cells spread along the polishing marks, especially on the disks after 4-day incubation. No difference was observed in the number of the cells on three disks after 1-, 4-, and 7-day incubations. No sign of corrosion such as discoloration, pitting, or precipitation of corrosion products were observed on all disks sterilized by UV-irradiation and autoclaving in naked eye.

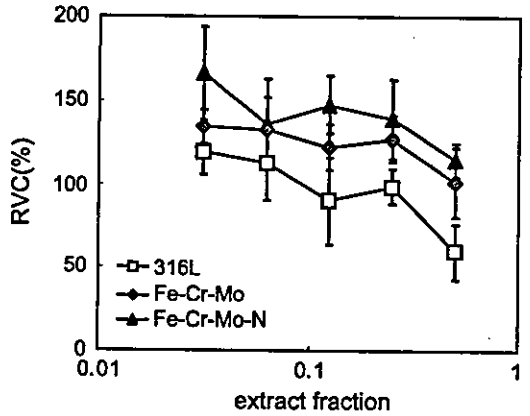

Fig. 5. Results of the cytotoxicity tests of 316L, Fe–Cr–Mo, and Fe–Cr–Mo–N in dynamic conditions. Relative viability of the cells (RVC) was calculated by the following equation: RVC (%)=$[(a-b)/(c-b)]\times 100$, where a was the absorbance of the sample well, b was the absorbance of the blank well, and c was the absorbance of the control well at 595 nm.

3.2. Cytotoxicity test in dynamic conditions

Cytotoxicity test of the extracts of three materials under wear conditions is shown in Fig. 5. On all of three disks, the RVC decreases when the fraction increases. However, the RVC of Fe–Cr–Mo–N was the highest among the three disks at all concentrations tested, followed by Fe–Cr–Mo.

3.3. Metallic elements in the extracts under dynamic conditions

The concentrations of each metallic element detected in the extracts of three materials after 14 days under dynamic conditions are shown in Table 2. In the extract of 316L, Ni was detected at the concentration of 14 ppb whereas Ni was not detected in the extracts of Fe–Cr–Mo–N. In the extract of Fe–Cr–Mo, Ni as well as Cr was detected at the concentration of 20 and 22 ppb, respectively.

Table 2
Quantification of metallic elements in the extracts

Samples	Metallic elements				
	Cr	Fe	Mn	Mo	Ni
316L	<10	<10	<10	<10	14
Fe–Cr–Mo	22	<10	–	<10	20
Fe–Cr–Mo–N	<10	<10	–	<10	<10

Unit: ppb(=ng/g); -: not analyzed.

4. Discussion

4.1. Cytotoxicity in static conditions

In this study, cytotoxicity evaluation in static conditions was performed for the disks sterilized in two ways; UV-irradiation and autoclaving. For Fe–Cr–Mo and Fe–Cr–Mo–N, no difference was observed in the two sterilization methods; both disks showed good cell growth. 316L, one of the conventional metallic biomaterials, showed different effect on cell proliferation depending on the sterilization methods. The disks of 316L sterilized by UV-irradiation inhibited cell proliferation whereas the disks sterilized by autoclaving did not inhibit it. In the cytotoxicity test in static conditions, two factors may influence cell growth on the disks: released metal ions from the disks and adsorbing protein onto the disks. The XPS analysis revealed that the composition of the surface oxide layer of 316L specimen is basically the same before and after autoclaving, that is, mixture of iron and chromium oxide [34]. This fact suggests that the behavior of adsorbing proteins does not differ between autoclaved and UV-irradiated disks of 316L. The thickness of the surface oxide layer of 316L specimen, however, increases by autoclaving [34], which will contribute to the higher corrosion resistance of the autoclaved specimen than polished, non-autoclaved one in cell culture condition. Furthermore, the concentration of nickel in the oxide layer is 0.3 (at.%) at autoclaved specimen whereas it is 0.5 (at.%) at polished, non-autoclaved one [34], which may reduce the amount of released nickel ion to cell culture medium. Therefore, the difference in the cell proliferation on 316L disks by sterilizing methods may be attributed to the difference of the corrosion resistance of the surface oxide as a passive film on the disks. As mentioned before, 316L has already been used in clinical cases as the devices for operation and medical treatment. Most of these devices are sterilized by autoclaving; therefore, the use of 316L in the clinical cases does not cause any trouble in the corrosion resistance and biocompatibility.

Concerning the nitrogen adsorption treatment, no difference was observed on cell growth between Fe–Cr–Mo and Fe–Cr–Mo–N disks despite the sterilization methods. This fact suggests that the nitrogen adsorption treatment has no effect on cytocompatibility in static conditions as well as the ferric stainless steel, Fe–Cr–Mo, has enough corrosion resistance and cytocompatibility in static conditions.

4.2. Cytotoxicity evaluation in dynamic conditions

In the dynamic conditions of this study, wear or fretting will occur at the interface between the disk and zirconia ball. Most of the implanting devices were used in dynamic conditions facing to the wear such as the sliding surface of an artificial joint and to the fretting (wear in small amplitude) such as the interface between the screw and the hole of the plate on bone fixing devices. It is well known that the wear and fretting accelerate the corrosion of metallic materials in a biological environment such as body fluid and cell culture medium [35–37]. Therefore, the cytotoxicity evaluation in static conditions is not enough to estimate the risks on biocompatibility of metallic materials for the devices facing to wear and fretting. Furthermore, the released metal ions in a small quantity can cause toxic reaction from cells [35,36]. In this study, the extraction of metal ions and debris from three kinds of disks was performed in dynamic conditions with cell culture medium at 37 °C. The extracting condition of this study is quite close to the actual environment of the implanted devices.

Cytotoxicity test of the extracts of Fe–Cr–Mo, Fe–Cr–Mo–N, and 316L resulted in the order of the inhibition of cell proliferation as 316L followed by Fe–Cr–Mo and Fe–Cr–Mo–N from the highest. The quantification of the metallic elements in the extracts revealed the release of Ni from 316L and Fe–Cr–Mo. These results indicate that Fe–Cr–Mo–N has superior cytocompatibility than the conventional metallic biomaterial, 316L. They also confirmed that the nitrogen adsorption treatment increases corrosion resistance of Fe–Cr–Mo with the existence of wear. The addition of nitrogen to a stainless steel influences the corrosion resistance of the steel; a solute nitrogen gives higher resistance to pitting and crevice corrosion whereas nitride accelerates intergranular corrosion [38]. In our previous study, the nitrogen adsorption treatment of Fe–Cr–Mo results in the change of its microstructure from ferrite to austenite without forming CrN or Cr_2N [16], giving higher Vickers hardness. These facts suggest that austenitization by adsorbed nitrogen contribute to higher corrosion and wear resistance, resulting in the higher cytocompatibility.

In the extracts of 316L, only Ni was detected whereas the content of Ni in 316L is much less than that of Cr. This suggests the preferential release of Ni from 316L under dynamic conditions in cell culture medium. The preferential release of Ni was also observed in Fe–Cr–Mo in which the nickel content is less than 0.01 mass%. The preferential release of Ni was reported on Ti–6Al–4V where the nickel is not contained as a component element but contained as impurity at the concentration less than 0.01 mass% [36]. Iron and chromium oxides are the main component of the surface oxide on 316L and Fe–23.5Cr–2Mo–1.5N (mass%) but small contents of nickel, molybdenum, and manganese oxides are also observed in the surface oxide layer [34,39]. However, the stability of nickel oxide is relatively low rather than chromium and other oxide, thus the preferential release of nickel could occur.

Though the concentration of released Ni in Fe–Cr–Mo extract is higher than that of 316L extract, the extract of Fe–Cr–Mo less inhibited cellular growth than that of 316L. One of the possible explanations is the Cr release in Fe–Cr–Mo extract. An addition of slight amount of Cr, which is one of the essential elements for human, may contribute to cell proliferation, resulting in higher cell growth of Fe–Cr–Mo than that of 316L.

5. Conclusions

Cytotoxicity tests of Fe–Cr–Mo, Fe–Cr–Mo–N, and 316L in static and dynamic conditions were performed to evaluate biocompatibility of Fe–Cr–Mo–N, a nickel-free austenitic stainless steel manufactured by nitrogen adsorption treatment and comparing to 316L, one of the conventional metallic biomaterials. As a result, Fe–Cr–Mo–N had higher cell growth than 316L in static and dynamic conditions. In dynamic conditions, the extract of Fe–Cr–Mo, which is the specimen before the nitrogen adsorption treatment, contained nickel, whereas no nickel was detected in the extract of Fe–Cr–Mo–N in dynamic conditions. This fact suggests that the nitrogen adsorption treatment contribute to the higher corrosion resistance of Fe–Cr–Mo–N in the presence of wear. Based on the results obtained in this study, Fe–Cr–Mo–N has a high possibility for the application in biomedical field; however, further research will be necessary to confirm its good biocompatibility in vivo.

References

[1] K. Hayashi, Biomaterial Sicence, in: JSME (Ed.), Ohmu-sha, Tokyo, 1993, p. 1.
[2] K. Nielsen, Br. Corros. J. 22 (1984) 272.
[3] P. Laffargue, H.J. Breme, J.A. Helsen, H.F. Hildebrand, Metals as biomaterials, in: J.A. Helsen, H.J. Breme (Eds.), John Wiley and Sons, Chichester, 1998, p. 467.
[4] K. Endo, K. Matsuda, Y. Abiko, H. Ohno, T. Kaku, Zairyo to Kankyo 46 (1997) 682.
[5] E. Tsuji, in: Y. Ikada (Ed.), Introduction for Biomaterials, Japan Scientific Societies Press, Tokyo, 1993, p. 125.
[6] A.B. Ferguson Jr., P.G. Laing, E.S. Hodge, J. Bone Jt. Surg. 42A (1960) 77.
[7] IARC Working Group on the Evaluation of Carcinogenic Risks to Humans, IARC Monographs on the Evaluation of Carcinogenic Risks to Humans, Chromium, Nickel and Welding, vol. 49, IARC, Lyon, 1990.
[8] S. Kawanishi, in: R.A. Goyer, G. Cherian (Eds.), Toxicology of Metals; Biochemical Aspects, Springer-Verlag, Berlin, 1995, p. 349.
[9] T.G. Rossman, Toxicology of Metals; Biochemical Aspects, in: R.A. Goyer, G. Cherian (Eds.), Springer-Verlag, Berlin, 1995, p. 373.
[10] I. Kimber, D.A. Basketter, in: L.W. Chang (Ed.), Toxicology of Metals, CRC Press, Boca Raton, 1996, p. 827.
[11] J. Menzel, W. Kirschner, G. Stein, ISIJ Int. 36 (1996) 893.
[12] P.J. Uggowizer, R. Magdowski, M.O. Speidel, ISIJ Int. 36 (1996) 901.
[13] R.C. Gebeau, R.S. Brown, Adv. Mater. Process. 159 (2001) 46.
[14] Y. Katada, M. Sagara, S. Iwasaki, K. Sakuraya, T. Kodama, Curr. Adv. Mater. Process. 13 (2000) 116.
[15] Y. Katada, H. Uno, M. Sagara, M. Ogawa, H. Baba, S. Iwasaki, K. Sakuraya, K. Hiroka, T. Kodama, C. Shiga, J. Mater. Process. Technol. 117 (2001) CD-ROM Section B1.
[16] D. Kuroda, T. Hanawa, T. Hibaru, S. Kuroda, M. Kobayashi, T. Kobayashi, Mater. Trans. 44 (2003) 414.
[17] H. Kawahara, A. Yamagami, M. Nakamura, Int. Dent. J. 18 (1968) 443.
[18] H. Kawahara, Bull. Jpn. Inst. Metals 31 (1992) 1033.
[19] M. Seyama, J. Jpn. Soc. Biomater. 8 (1990) 73.
[20] M. Kaga, M. Onogi, M. Ohta, J. Jpn. Soc. Biomater. 2 (1984) 117.
[21] H. Kobayashi, J. Jpn. Soc. Biomater. 2 (1984) 165.
[22] M. Nakamura, Y. Kawada, H. Sakae, S. Saeki, K. Imai, H. Kawahara, Shikai Tenbo 64 (1984) 451.
[23] S. Yoshioka, J. Jpn. Dent. Mater. Devices 8 (1989) 324.
[24] S. Takeda, H. Kosugi, K. Takimoto, N. Tsutsumi, M. Nakamura, J. Jpn. Dent. Mater. Devices 9 (1990) 825.
[25] J.C. Wataha, C.T. Hnaks, R.G. Craig, J. Biomed. Mater. Res. 25 (1991) 1133.
[26] J.C. Wataha, C.T. Hanks, R.G. Craig, J. Biomed. Mater. Res. 28 (1994) 427.
[27] A. Shedle, P. Samorapoompichit, X.H. Rausch-Fan, A. Franz, W. Fureder, W.R. Sperr, W. Sperr, A. Ellinger, R. Slavicek, G. Boltz-Nitulescu, P. Valent, J. Dent. Res. 74 (1995) 1513.
[28] T. Rae, J. Bone Jt. Surg. 57B (1975) 444.
[29] T. Rae, J. Bone Jt. Surg. 63B (1981) 435–440.
[30] M.J. Maloney, R.L. Smith, F. Castro, D.J. Schuman, J. Bone Jt. Surg. 75A (1993) 835.
[31] W.J. Maloney, F. Castro, D.J. Schurman, R.L. Smith, J. Appl. Biomater. 5 (1994) 109.
[32] T. Sasada, T. Imaizumi, M. Morita, K. Mabuchi, Junkatsu 33 (1988) 288.
[33] A.M. Pappas, J. Cohen, J. Bone Jt. Surg. 50A (1968) 535.
[34] T. Hanawa, S. Hiromoto, A. Yamamoto, D. Kuroda, K. Asami, Mater. Trans. 43 (2002) 3088.
[35] A. Yamamoto, T. Kobayashi, N. Maruyama, M. Sumita, J. Jpn. Soc. Biomater. 14 (1996) 158.
[36] A. Yamamoto, T. Kobayashi, N. Maruyama, K. Nakazawa, M. Sumita, J. Jpn. Inst. Metals 59 (1995) 463.
[37] H. Doi, S. Takeda, J. Jpn. Dent. Mater. Devices 9 (1990) 375.
[38] K. Osozawa, Netsu Shori 36 (1996) 206.
[39] D. Kuroda, T. Hanawa, S. Hiromoto, Y. Katada, K. Asami, Mater. Trans. 43 (2002) 3093.

Materials Transactions, Vol. 45, No. 1 (2004) pp. 112 to 118

Torsion and Tensile Properties of Thin Wires of Nickel-Free Stainless Steel with Nitrogen Absorption Treatment

Daisuke Kuroda[1], Takao Hanawa[1], Takaaki Hibaru[2], Syuji Kuroda[2] and Masaki Kobayashi[2]

[1]*Biomaterials Center, National Institute for Materials Science, Tsukuba 305-0047, Japan*
[2]*Steel Research Center, National Institute for Materials Science, Tsukuba 305-0047, Japan*

A new manufacturing process for nickel-free austenitic stainless steel has been developed by authors. In combination with machining and a nitrogen absorption treatment, this process makes it possible to form small precise devices with a maximum thickness or diameter of 4 mm. The refinement of grains of Fe-24Cr-2Mo in mass% was attempted by thermo-mechanical treatment before nitrogen absorption treatment in order to increase the mechanical properties after nitrogen absorption treatment. Torsion and tensile properties and microstructures of Fe-24Cr-2Mo before and after nitrogen absorption treatment were evaluated to understand the effects of grain refinement on nitrogen absorption. The thin wire of the alloy is completely austenitized with nitrogen absorption at 1473 K for over 7.2 ks. The mean grain size of the alloy with nitrogen absorption decrease with the grain refinement process attempted in this study. The values of ultimate tensile strength and elongation in the alloy with and without nitrogen absorption increase with the grain refinement process. The torsional stress and rotation angle to fracture of the alloy increase with the grain refinement process and nitrogen absorption. According to the results of the torsion and tensile tests, the thin wire of the alloy with nitrogen absorption is expected to have good mechanical properties than conventional austenitic stainless steels.

(Received July 22, 2003; Accepted November 5, 2003)

Keywords: *nickel-free austenitic stainless steel, nitrogen absorption, thin wire, grain refinement, torsion properties, tensile properties*

1. Introduction

A new manufacturing process for nickel-free austenitic stainless steel has been developed by authors.[1)] In combination with machining and a nitrogen absorption treatment, this process makes it possible to form small precise devices with a maximum thickness or diameter of 4 mm.[1)] Ingot of ferritic stainless steel, Fe-24Cr-2Mo in mass%, is worked to various dimensions such as round bar, thin plate, and thin wire.[1-3)] The balance between strength and elongation in each test specimen with nitrogen absorption is the same as that in conventional austenitic stainless steel such as 316L.

However, the temperature for nitrogen absorption, 1473 K, is sufficiently high for grain growth, and the coarsening is observed after nitrogen absorption.[1-3)] The grain growth and coarsening causes decrease in the mechanical properties. Therefore, a nitrogen absorption treatment that allows the retention of strength and ductility is performed with a grain refinement process before nitrogen absorption treatment.

In this study, we attempted the refinement of grains by thermo-mechanical treatment before nitrogen absorption treatment in order to increase the mechanical properties after nitrogen absorption treatment. The torsion and tensile properties and microstructures of Fe-24Cr-2Mo in mass% with fine grains generated by hot forging and cold forging were evaluated both before and after nitrogen absorption treatment to understand the effects of grain refinement on nitrogen absorption. The results were compared to those of the alloy in the previous study[1-3)] and conventional austenitic stainless steel.

2. Experimental Procedure

2.1 Specimen preparation

Ingot with 20 kg of Fe-24Cr-2Mo in mass% was prepared by a vacuum high-frequency induction melting process. Table 1 shows the chemical composition of the alloy. The ingot was then cut into three equal parts. Figure 1 shows a schematic diagram of the forging process. Hot radial forging, followed by 99% cold radial forging, was conducted in the previous study.[3)] In this study, 84% hot radial forging and 99.99% cold radial forging were conducted to obtain finer grains than in the previous study.[3)] Thin wires (1.0 mm in diameter) were obtained through hot and cold radial forging. Specimens for the torsion and tensile tests (1.0 mm in diameter and 10 mm in gage length) and hardness test (1.0 mm in diameter and 10 mm in length) were prepared from the thin wires. The tensile axis was along to the radial forging direction in specimens for the tensile test.

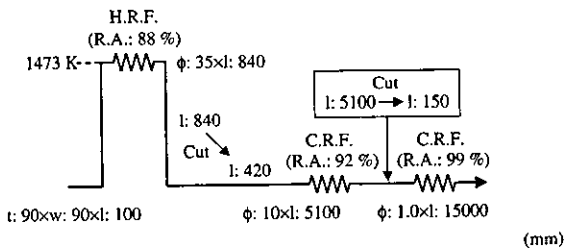

Fig. 1 Schematic diagram of the forging process of a thin wire. H.F.: hot forging, C.F.: cold forging, R.A.: reduction of area, *t*: thickness, *w*: width, *ϕ*: diameter, and *l*: length.

Table 1 Chemical composition of Fe-24Cr-2Mo (mass%).

C	Mn	P	S	Si	Ni	Cr	Mo	O	N	Fe
0.002	<0.01	<0.002	0.0002	<0.01	<0.01	25.80	2.04	0.016	<0.001	Bal.

2.2 Nitrogen absorption

Specimens for the torsion, tensile, and hardness tests of the alloy were polished with #600 SiC paper in water and then ultrasonically rinsed in acetone for 300 s. After rinsing, the specimens were separately located to a 304 steel reticular stage. The area for nitrogen absorption in the specimens did not contact the stage. The stage with the specimens was inserted into the nitrogen absorption furnace.[1-3] The pressure of the inside of the furnace was reduced to 2 Pa, and nitrogen gas (<99.99%) was introduced and continuously flew into the furnace to maintain a pressure of 101.3 kPa. The temperature of the furnace was increased from ambient to 1473 K at a rate of 0.08 K s^{-1} and kept for 7.2 ks, 10.8 ks, 14.4 ks, 18.0 ks, and 21.6 ks. Immediately after heating, the specimens were quenched into a water bath. The scale generated on each specimen was removed with #600 SiC paper in water after nitrogen absorption.

2.3 Examination of microstructure and mechanical properties

Gripped parts of torsion test specimens were employed for microstructural observation. Specimens for microstructural examination and hardness test were finally polished with #600 SiC paper and buffed. After etching with a Villela reagent, the microstructure was observed with an optical microscope. Phases of specimens for the torsion test with and without nitrogen absorption were identified using X-ray diffractometry (XRD) with CuKα radiation (40 kV and 300 mA). The hardness test was performed using a micro Vickers hardness tester. The torsion test was performed in air using a torsion testing machine with a capacity of 0.2 N as shown in Fig. 2. The rotation speed of gripped part was 0.1 Hz. Torque and rotation angle to fracture were estimated throughout the torsion test. The torsional stress, τ was calculated by the following equation:

$$\tau\ (\mathrm{N/m^2 = Pa}) = T\ (\mathrm{N{\cdot}m})/Z_p\ (\mathrm{m^3}) \quad (1)$$

where T is the torque and Z_p is the polar modulus of section. The polar modulus of section, Z_p, was calculated by the following equation:

$$Z_p\ (\mathrm{m^3}) = \pi d^3/16 \quad (2)$$

where d is the diameter of the specimen for torsion test.

Tensile tests were performed in air using an Instron-type tensile testing machine with a capacity of 10 kN. The crosshead speed was 8.33×10^{-6} m s^{-1}. Ultimate tensile strength, 0.2% proof stress, and elongation to fracture were estimated throughout the tensile test. At least, three measurements were carried out under the same conditions, and the mean values were calculated. The fractured surfaces were observed with a scanning electron microscope (SEM) after torsion and tensile tests.

For comparison, changes in phases, hardness and torsion and tensile properties that were the result of heating without nitrogen absorption were investigated by heating under the same temperature and time as the nitrogen absorption treatment in an argon atmosphere.

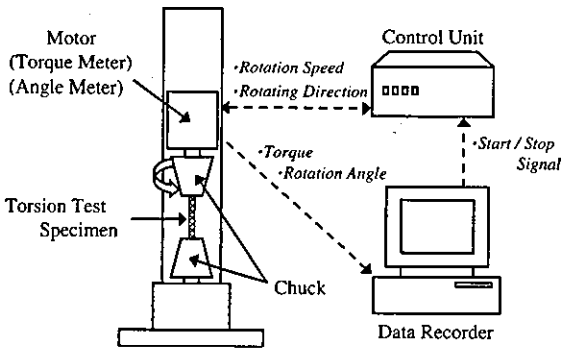

Fig. 2 Schematic illustration of the torsion test system.

3. Results and Discussion

3.1 Changes in microstructures by nitrogen absorption

XRD profiles of Fe-24Cr-2Mo with and without nitrogen absorption and Fe-24Cr-2Mo heated at 1473 K in an argon atmosphere are shown in Fig. 3. Only diffraction pattern of ferrite (α phase) was observed from Fe-24Cr-2Mo without nitrogen absorption and Fe-24Cr-2Mo heated at 1473 K in an argon atmosphere (Figs. 3(a) and (b)), indicating that phase transformation from α phase to austenite (γ phase) does not occur in an argon atmosphere. On the other hand, only peaks originating from γ phase were observed from the alloy with nitrogen absorption for over 7.2 ks, indicating that the thin wire of the alloy is completely austenitized with nitrogen absorption treatment for 7.2 ks (Fig. 3(a)). Using XRD, neither CrN nor Cr_2N was identified in any specimen with nitrogen absorption, indicating that precipitation of nitride

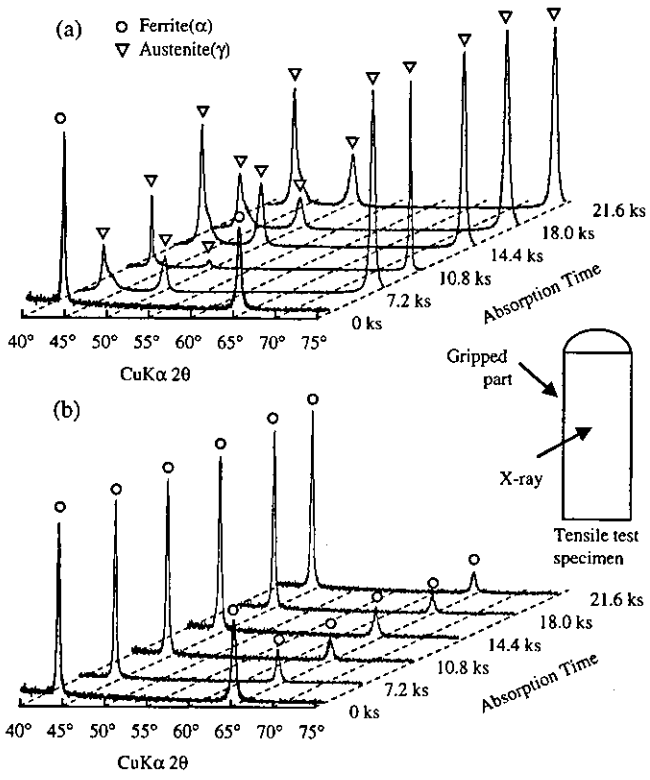

Fig. 3 X-ray diffraction patterns of (a) Fe-24Cr-2Mo with and without nitrogen absorption and (b) Fe-24Cr-2Mo heated at 1473 K in an argon atmosphere.

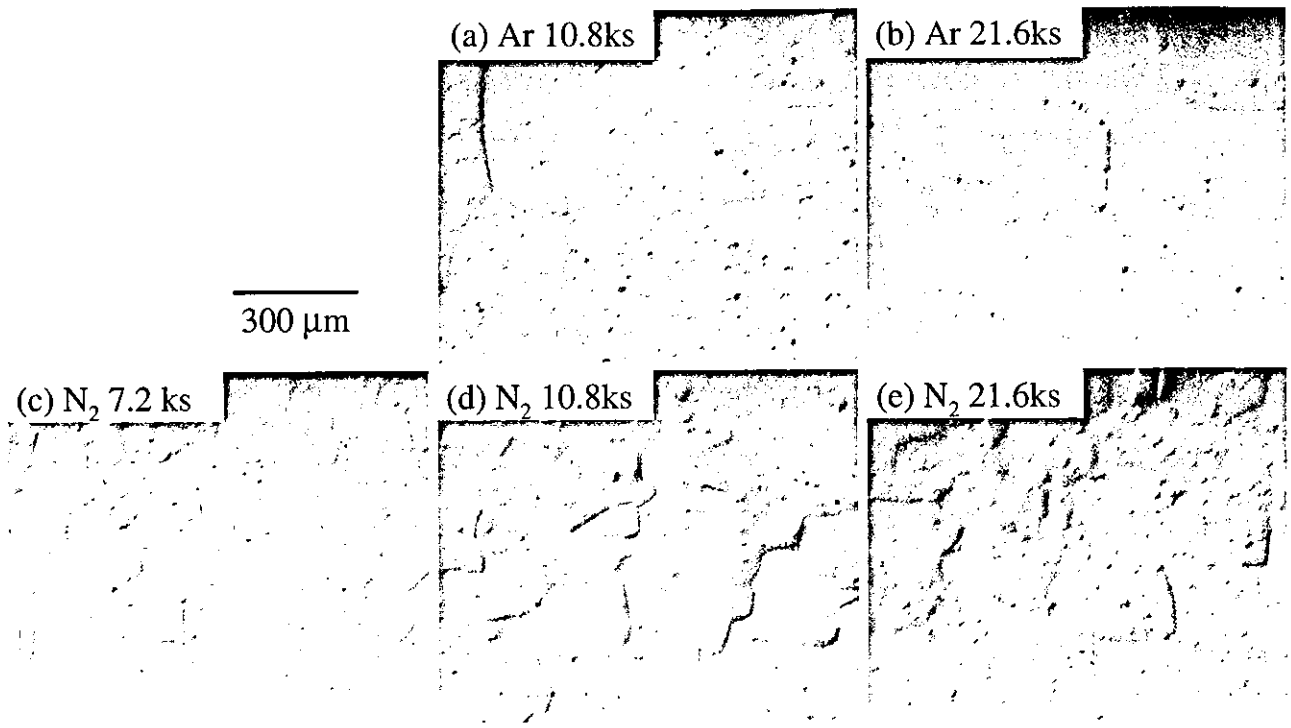

Fig. 4 Optical microstructure of Fe-24Cr-2Mo in each treatment. (a) and (b) heated at 1473 K in an argon atmosphere, and (c), (d) and (e) heated at 1473 K in a nitrogen atmosphere.

does not occur in Fe-24Cr-2Mo with nitrogen absorption. The result of XRD in this study is in good agreement with that in the previous study.[1-3)]

The microstructures of Fe-24Cr-2Mo with nitrogen absorption and Fe-24Cr-2Mo heated in an argon atmosphere are shown in Fig. 4. The microstructures of the alloy before nitrogen absorption and heat treatment in an argon atmosphere were a fine α phase expanded along the radial forging direction. The α phase was only observed in Fe-24Cr-2Mo heated in an argon atmosphere (Figs. 4(a) and (b)). Fine grains in Fe-24Cr-2Mo were grown and coarsened with the nitrogen absorption treatment and heat treatment in an argon atmosphere. The mean grain size of the alloy after heated for 21.6 ks in an argon atmosphere was 433 μm. The grains were the largest with 21.6-ks nitrogen absorption (Fig. 4(e)). The mean grain size of the alloy after 21.6-ks nitrogen absorption was 126 μm. The mean grain size of the alloy slightly increased with increasing nitrogen absorption time. The grain size of Fe-24Cr-2Mo heated in an argon atmosphere was much larger than that of the alloy with nitrogen absorption, indicating that nitrogen works as a strong inhibitor against the coarsening. In addition, that of the alloy after 21.6-ks nitrogen absorption and heated for 21.6 ks in an argon atmosphere in the previous study was 132 μm and 527 μm, respectively.[3)] The grain size of the alloy in this study was smaller than that in the previous study,[3)] indicating that the resultant grain in the alloy was refined with the grain refinement process attempted in this study.

3.2 Changes in hardness by nitrogen absorption

The changes in micro Vickers hardness of Fe-24Cr-2Mo with and without nitrogen absorption treatment and the alloy heated in an argon atmosphere are shown in Fig. 5. For comparison, that of the alloy with and without nitrogen absorption treatment and heated in an argon atmosphere in the previous study[3)] is also shown. Although the micro Vickers hardness of the alloy after annealing was 150, that of thin wire of the alloy after 99.99% cold forging was 280 because of work hardening. The hardness of the alloy without nitrogen absorption in this study was the same as that in the

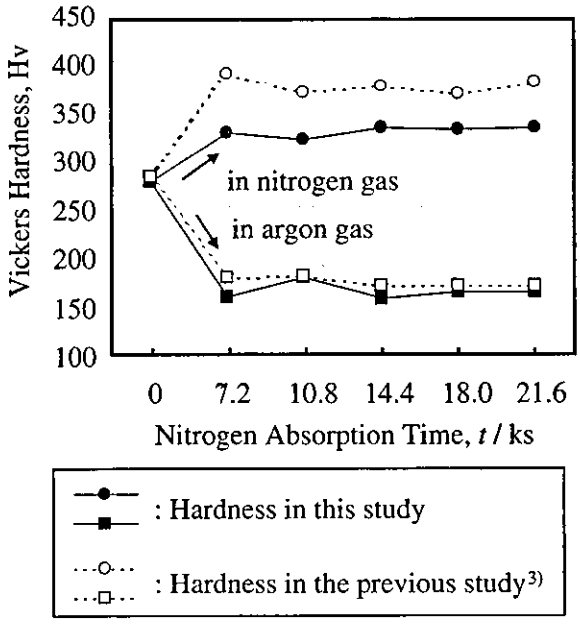

Fig. 5 Comparison of the micro Vickers hardness of Fe-24Cr-2Mo with and without nitrogen absorption and Fe-24Cr-2Mo heated at 1473 K in an argon atmosphere. For comparison, that of the alloy with and without nitrogen absorption treatment and heated in an argon atmosphere in the previous study[3)] is also shown.

previous study. However, the hardness of the alloy with nitrogen absorption in this study was smaller than that in the previous study. On the other hand, the hardness of the alloy heated in an argon atmosphere in this study was the same as that in the previous study. The hardness of Fe-24Cr-2Mo increased with 7.2-ks nitrogen absorption, and the value was maintained when the duration of the nitrogen absorption was extended. The hardness of the alloy showed the maximum value (Hv=337) at 21.6-ks nitrogen absorption. On the other hand, the hardness decreased in an argon atmosphere with heating for 7.2 ks. This indicates that the release of residual stress by heat treatment in an argon atmosphere.

3.3 Changes in tensile properties by nitrogen absorption

Figure 6 shows the ultimate tensile strength, 0.2% proof stress, elongation to fracture, and reduction of area of Fe-24Cr-2Mo with and without nitrogen absorption treatment and Fe-24Cr-2Mo heated in an argon atmosphere. The tensile strength, 0.2% proof stress, and reduction of area of the alloy decreased with nitrogen absorption, while elongation to fracture of the alloy increased with nitrogen absorption. Elongation to fracture of the alloy increased with increasing nitrogen absorption time. The value of tensile strength of the alloy with nitrogen absorption is much larger than that of 0.2% proof stress of the alloy with nitrogen absorption, indicating that magnitude of work-hardening increased with solid-solution strengthening of nitrogen. Fe-24Cr-2Mo with nitrogen absorption for 14.4 ks showed maximum ultimate tensile strength (1033 MPa). Elongation to fracture of the alloy showed the maximum value (65%) at 21.6-ks nitrogen absorption. The maximum values of tensile strength and elongation obtained from the alloy with nitrogen absorption in this study are larger than those of the alloy with nitrogen absorption in the previous study (985 MPa and 41%).[3] In this study, the amounts of nitrogen in the thin wires of Fe-24Cr-2Mo at 7.2-ks and 21.6-ks absorption were 0.92 mass% and 0.95 mass%, respectively. The amount of nitrogen in the thin wire of the alloy increased with 7.2-ks nitrogen absorption, and the amount was maintained when the duration of the nitrogen absorption was extended. On the other hand, the amounts of nitrogen of the thin wires of Fe-24Cr-2Mo at 7.2-ks and 21.6-ks absorption were 0.92 mass% and 0.93 mass% in the previous study. The amount of nitrogen of the alloy with nitrogen absorption in this study was the same as that in the previous study. Therefore, tensile properties of the alloy with nitrogen absorption in this study improved with the grain refinement process attempted in this study. The tensile strength and 0.2% proof stress decreased and elongation to fracture and reduction of area increased with a heat treatment in an argon atmosphere. The hardness of the cold-forged Fe-24Cr-2Mo was also decreased with the heat treatment (Fig. 5). These results suggest the residual stress was released by the heat treatment. Fe-24Cr-2Mo heated at 1473 K for 21.6 ks in an argon atmosphere showed maximum ultimate tensile strength and elongation to fracture, 310 MPa and 19%, respectively. The tensile strength and elongation to fracture obtained from the alloy heated in an argon atmosphere in this study are the same as those of the alloy heated in an argon atmosphere in the previous study.[3] The tensile strength,

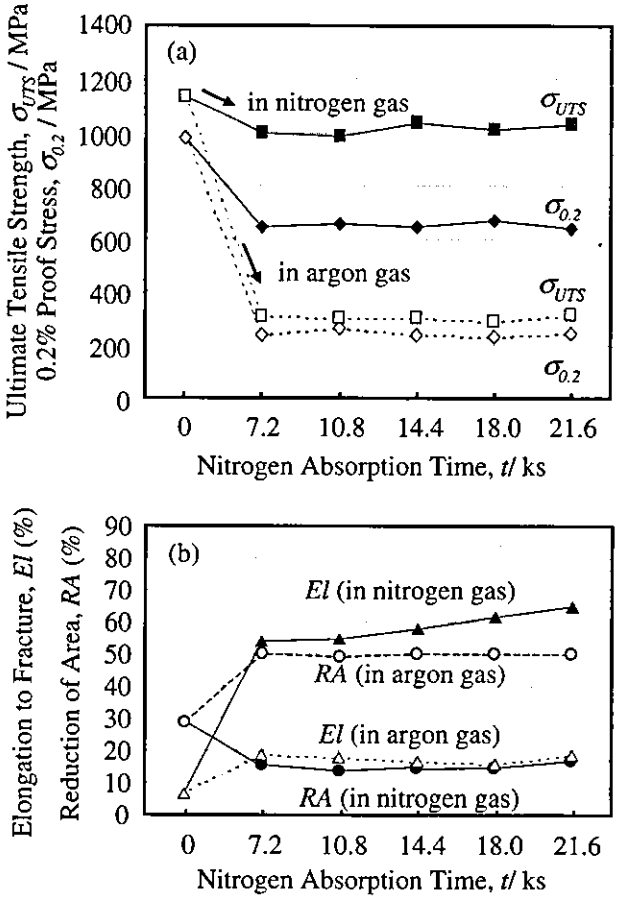

Fig. 6 (a) Ultimate tensile strength and 0.2% proof stress and (b) elongation to fracture and reduction of area of Fe-24Cr-2Mo with and without nitrogen absorption and Fe-24Cr-2Mo heated at 1473 K in an argon atmosphere.

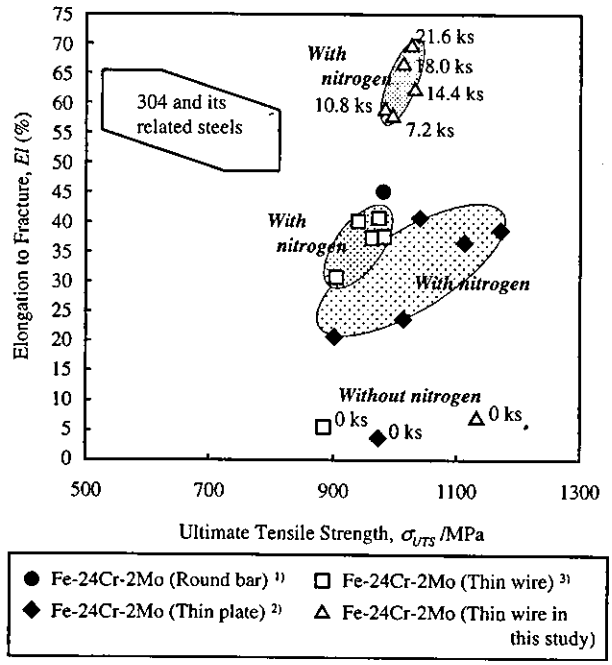

Fig. 7 Ultimate tensile strength and elongation to fracture of Fe-24Cr-2Mo with and without nitrogen absorption and of conventional austenitic stainless steels.

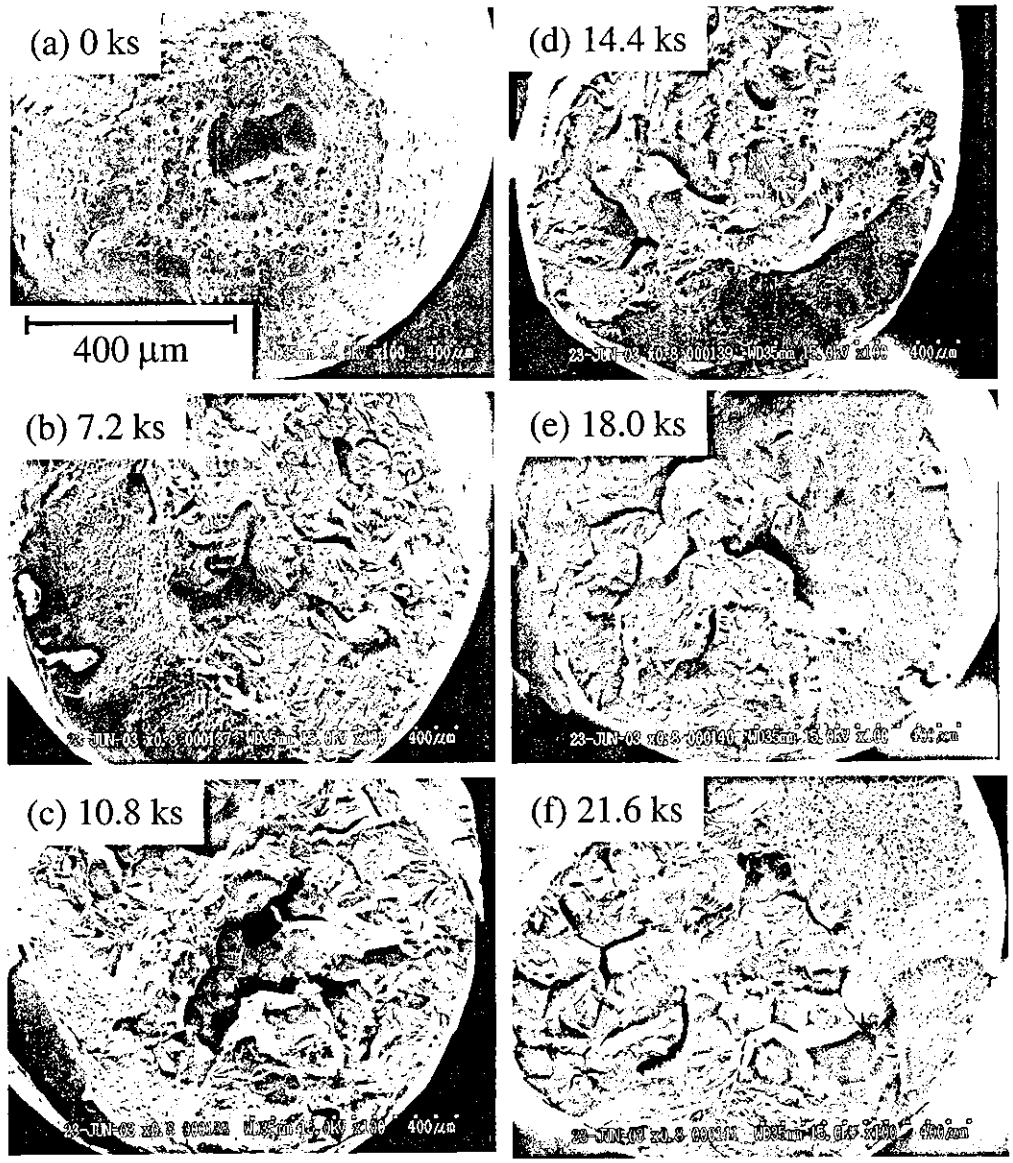

Fig. 8 Scanning electron micrographs of fractured surfaces of Fe-24Cr-2Mo with nitrogen absorption for (a) 0 ks, (b) 7.2 ks, (c) 10.8 ks, (d) 14.4 ks, (e) 18.0 ks, and (f) 21.6 ks after tensile test.

0.2% proof stress, and elongation to fracture of the alloy with nitrogen absorption were larger than those of the alloy heated in an argon atmosphere.

The relation between ultimate tensile strength and elongation to fracture of Fe-24Cr-2Mo with and without nitrogen absorption is shown in Fig. 7. The figure also contains the data on a round bar, thin plate, and thin wire of Fe-24Cr-2Mo with nitrogen absorption and 316L steel previously reported.[1-3] The best balance between strength and elongation was given by 21.6-ks nitrogen absorption in Fe-24Cr-2Mo, and the balance was larger than that in the thin wire in the previous study[3] and conventional austenitic stainless steel.[1] However, the balance between strength and elongation of thin wire of the alloy with nitrogen absorption was lower than that of the thin plate in the previous study.[2]

Figure 8 shows the scanning electron micrographs of fractured surfaces of Fe-24Cr-2Mo with and without nitrogen absorption treatment. Specimen without nitrogen absorption shows a ductile fracture surface (Fig. 8(a)). Fe-24Cr-2Mo with nitrogen absorption specimens showed good elongation (Fig. 6(b)), whereas the fractured surface of specimens with nitrogen absorption showed a brittle fracture surface. The addition of nitrogen reduces the formability because it increases the brittleness of the γ phases.[4] In addition, the grain boundary cracks generate during cold rolling in a highly nitrogen contained (0.9 mass%) Fe-Cr-Mn-N steel.[5] Over 0.9 mass% nitrogen can be absorbed by Fe-24Cr-2Mo with nitrogen absorption treatment.[1] Therefore, the brittle fractures observed in the alloy with nitrogen absorption were caused by brittleness of the γ phase.

The tensile strength of Fe-24Cr-2Mo is governed by the refinement of grains, according to the results of microstructural observations, tensile test, and observation of fractured surface.

3.4 Changes in torsion properties by nitrogen absorption

Figure 9 shows the torsional stress and rotation angle to

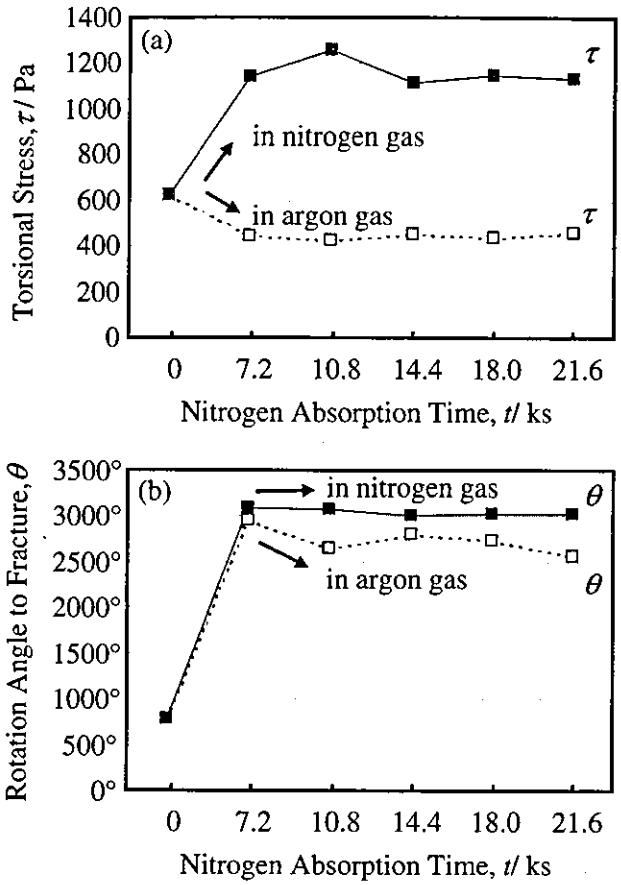

Fig. 9 (a) Torsional stress and (b) rotation angle to fracture of Fe-24Cr-2Mo with and without nitrogen absorption and Fe-24Cr-2Mo heated at 1473 K in an argon atmosphere.

fracture of Fe-24Cr-2Mo with and without nitrogen absorption and Fe-24Cr-2Mo heated in an argon atmosphere. The torsional stress and rotation angle to fracture of the alloy increased with nitrogen absorption. Fe-24Cr-2Mo with nitrogen absorption for 14.4 ks showed maximum torsional stress (1258 Pa). Rotation angle to fracture of the alloy showed the maximum value (3094°) at 7.2-ks nitrogen absorption. On the other hand, the torsional stress of the alloy decreased and rotation angle to fracture increased with a heat treatment in an argon atmosphere. Fe-24Cr-2Mo with heated for 21.6 ks showed maximum torsional stress (465 Pa). Rotation angle to fracture of the alloy showed the maximum value (2964°) at 7.2-ks heat treatment in an argon atmosphere. The torsional stress and rotation angle to fracture of the alloy with nitrogen absorption were larger than those of the alloy with heating in an argon atmosphere. Therefore, torsion properties of the alloy increased with nitrogen absorption.

Figure 10 shows the relation between torsional stress and rotation angle to fracture of the alloy with and without nitrogen absorption and that of the thin wire of 316L steel in annealed condition. The balance between torsional stress and rotation angle to fracture of the alloy increased with nitrogen absorption. The balance between torsional stress and rotation angle to fracture of the alloy with nitrogen absorption was larger than that of the annealed 316L steel, while that of the alloy with a heating in an argon atmosphere as smaller than that of 316L steel. The best balance between torsional stress

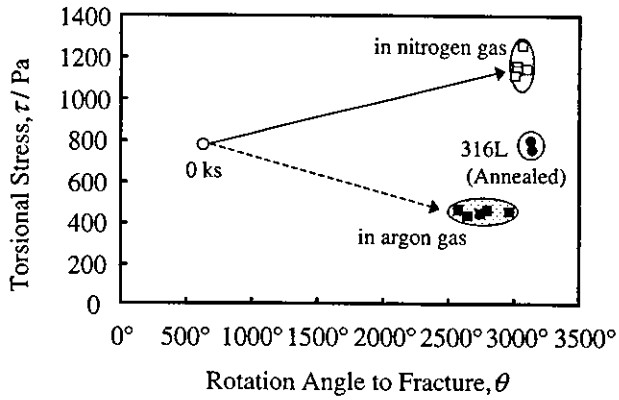

Fig. 10 Torsional stress and rotation angle to fracture of Fe-24Cr-2Mo with and without nitrogen absorption and of conventional austenitic stainless steel.

and rotation angle to fracture was given by 18.0-ks nitrogen absorption in Fe-24Cr-2Mo, and the balance was larger than that in 316L.

4. Conclusions

The refinement of grains of Fe-24Cr-2Mo in mass% was attempted by thermo-mechanical treatment before nitrogen absorption treatment in order to increase the mechanical properties after nitrogen absorption treatment. Torsion and tensile properties and microstructures of Fe-24Cr-2Mo before and after nitrogen absorption treatment were evaluated to understand the effects of grain refinement on nitrogen absorption. The results obtained are as follows:

(1) The mean grain size of Fe-24Cr-2Mo with nitrogen absorption decrease with the grain refinement process attempted in this study.

(2) The tensile properties of the alloy with nitrogen absorption in this study improved with the grain refinement process attempted in this study. The best balance between strength and elongation is given by 21.6-ks nitrogen absorption in Fe-24Cr-2Mo, and the balance was larger than that in conventional austenitic stainless steel.

(3) The torsion properties of the alloy increase with the grain refinement process and nitrogen absorption. The balance between torsional stress and rotation angle to fracture in Fe-24Cr-2Mo with nitrogen absorption at 1473 K for over 7.2 ks is larger than that in conventional austenitic stainless steel.

(4) The thin wire of the alloy with nitrogen absorption is expected to have good mechanical properties than conventional austenitic stainless steels.

Acknowledgements

We would like to thank Mr. Kenshi Morita, Mr. Hironori Kawasaki and Mr. Morihide Makino for their valuable support during the experiments.

REFERENCES

1) D. Kuroda, T. Hanawa, T. Hibaru, S. Kuroda, M. Kobayashi and T. Kobayashi: Mater Trans. **44** (2003) 414-420.
2) D. Kuroda, T. Hanawa, T. Hibaru, S. Kuroda, M. Kobayashi and T. Kobayashi: Mater Trans. **44** (2003) 1363-1369.
3) D. Kuroda, T. Hanawa, T. Hibaru, S. Kuroda, M. Kobayashi and T. Kobayashi: Mater Trans. **44** (2003) 1557-1582.
4) G. Stain and J. Menzel: Stahl Eisen **112** (1992) 47-52.
5) K. Kataoka, T. Tsuchiyama, H. Goto and S. Takaki: J. Jpn. Soc. Powder Metallurgy **46** (1999) 922-926.

B5−3

生体用Niフリーステンレス鋼の開発

（物質・材料研究機構　生体材料研究センター）○黒田大介

1．緒　言

金属系医療用デバイスの素材として，素材価格が安く，優れた加工性を有するオーステナイト型ステンレス鋼（316L鋼）が主に使用されている。しかし，316L鋼に含まれるNiは金属アレルギーの原因物質として問題視されていることから，Niのかわりに高濃度のNを添加した高濃度窒素含有オーステナイト型ステンレス鋼（以下，Niフリーステンレス鋼）の開発がEU諸国を中心に精力的に進められている。一方，アジア地域におけるNiフリーステンレス鋼の研究・開発は日本以外では行われていない。これは，金属アレルギーは黄色人種には少ないため，Niのアレルギー性がEU諸国ほど問題視されていないからである。また，高濃度のNを含むNiフリーステンレス鋼は生体用金属材料として優れた特性を示すが，溶解，成形加工などに特殊な設備や技術が必要であり，加工条件によっては素材が非常に脆くなってしまうため，Niフリーステンレス鋼のインゴットから医療用デバイスや民生品を安価かつ簡便に製造する技術は未だ開発されていない。これらの問題がNiフリーステンレス鋼の実用化を困難にしている。

そこで，これまでの生体用Niフリーステンレス鋼の研究開発動向を概説するとともに，Niフリーステンレス鋼製の製品を安価かつ簡便に製造するために演者らが開発した“成形加工と窒素吸収処理を組み合わせたNiフリーステンレス鋼製品の製造技術”について紹介する。さらに，開発した技術で製造したNiフリーステンレス鋼の力学的特性，耐食性，生体適合性などについても紹介し，Niフリーステンレス鋼の生体，民生分野への適用の可能性，新しい製造技術の実用の可能性について述べる。

2．生体用Niフリーステンレス鋼の研究開発動向

高濃度窒素含有オーステナイト型ステンレス鋼は，もともと海洋構造物材料として開発された合金である。これら合金には耐塩化物腐食性，耐隙間腐食性，耐孔食性を改善させるためにN，Mn，Niが複合添加される。EU諸国で開発された生体用Niフリーステンレス鋼には力学的強度や耐食性を改善するためにNやMnが複合添加される傾向があるが，Mnの発癌性も近年報告されていることから，日本ではNiだけでなくMnも含まない生体用Niフリーステンレス鋼が開発されている。NiやMnはオーステナイト形成元素であるため，これら元素の添加量の減少にともないN添加量を増加させる必要がある。0.3 mass%以上のNをステンレス鋼に添加するために，加圧ESR(Electro Slag Remelting)法という特殊な溶解技術が使用される。しかし，加圧ESR法では成分設計に制約が多く，さらに消耗電極の製造にコストがかかるため，素材は非常に高価になる。また，加圧ESR法で製造した素材は非常に硬いため，成形や機械加工によってインゴットから直接製品を製造することは困難である。

3．新しいNiフリーステンレス鋼の製造技術

Nを含まない軟らかいフェライト型ステンレス鋼の状態で製品形状に加工し，最終製品にNを吸収させることで形状を変化させることなく製品全体をオーステナイト組織化する製造技術を開発した。窒素を含まないFe-24Cr-2Mo (mass%)合金において厚さ200μmの箔材や直径350μmの線材が容易に成形できること，開発した技術で0.9 mass%以上のNを含む直径あるいは厚さが最大で4 mmのNiフリーステンレス鋼製品を製造できることなどを確認している。また，N吸収したNiフリーステンレス鋼は，優れた細胞適合性，組織適合性を有することも確認している。現在，種々の製品の試作を行っている（Fig. 1）。

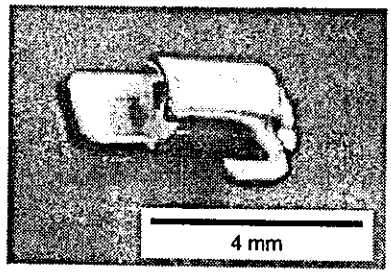

Fig. 1 試作したバッカルチューブ

Development of Nickel-free Stainless Steel for Biomedical applications
(Biomaterials Research Center, Nationals Institute for Materials Science.)
D. KURODA
Tel: 029-860-4179 FAX: 029-860-4715, E-mail: KURODA.Daisuke@nims.go.jp

(36)

窒素吸収処理したNiフリーステンレス鋼の生体親和性

（物・材機構　生体材料研究センター）　○黒田大介
（北海道大学大学院歯学研究科）　横山敦郎
（物・材機構　生体材料研究センター）　山本玲子，塙　隆夫，廣本祥子

【はじめに】 我々は、窒素吸収処理を利用したNiフリーステンレス鋼の新しい製造技術を開発した。この技術により、発癌性・アレルギー性が指摘されているNiを添加することなく高い力学的強度、耐食性および細胞適合性を有する小型のNiフリーステンレス鋼製品を製造できる。本研究では、新技術で製造したNiフリーステンレス鋼の生体親和性をラットモデルにより評価し、既存の生体用金属材料である純チタンおよびSUS316L鋼と比較した。

【実験方法】新技術で製造した直径1 mmのFe-24Cr-2Mo-1N (mass%)ワイヤー、市販の直径1 mmの純チタン胸骨針ワイヤーおよび直径0.8 mmのSUS316L鋼胸骨針ワイヤーを供試材とした。それらワイヤーをそれぞれ長さ5 mmに切断後、切断部のみを#2000までのエメリー紙により湿式研磨した。さらにアセトンおよびアルコールで洗浄、オートクレーブ滅菌し、生後12週齢雄のウィスター系ラットの左側大腿骨に2本、腹部皮下組織に1本埋入した。1週および4週間埋入した後に、試料を周辺組織とともに摘出した。周辺組織から試料を除去して標本を作製し、HE染色後に観察した。

【結　果】 皮下組織に埋入したSUS316L鋼の周辺組織では腐食生成物が認められたが、Fe-24Cr-2Mo-1Nおよび純チタンを埋入した部位の周辺組織では腐食生成物は認められなかった。また、骨組織に埋入したFe-24Cr-2Mo-1Nおよび純チタンの表面では、線維性結合組織を介することなく新生骨が形成された。以上の結果から、Fe-24Cr-2Mo-1NはSUS316L鋼よりも優れた生体親和性および骨伝導性を有することが明らかとなった。